On the modeling of urban air mobility vehicle takeoff and landing operations in the FAA Aviation Environmental Design Tool

Stefan J. Letica[1], Stephen A. Rizzi[2]
NASA Langley Research Center
Hampton, VA 23681

ABSTRACT

Urban air mobility (UAM) vehicles are anticipated to operate in close proximity to the public. A possible barrier to the introduction of UAM vehicles as a transit solution is their community noise impact, particularly around vertiports. The Federal Aviation Administration Aviation Environmental Design Tool (AEDT) is the mandated tool to assess aircraft noise and other environmental impacts due to federal actions at civilian airports, vertiports, or in U.S. airspace for commercial flight operations. However, AEDT was designed to model fixed-wing aircraft and conventional helicopter operations, not UAM vehicles. Prior work by the authors showed significant differences in noise contours of UAM departures and approaches when modeling operations as fixed-wing and helicopter types in AEDT. This paper identifies the sources of those differences. Additionally, a NASA time-marching simulation tool is used to generate noise exposure predictions for equivalent operations to help identify differences associated with the noise model implemented in AEDT and offer possible changes to assess UAM community noise impact more consistently with simulation-based modeling.

1. INTRODUCTION

In the United States, the Federal Aviation Administration (FAA) Aviation Environmental Design Tool (AEDT) [1] is the required tool to assess aircraft noise and other environmental impacts due to federal actions at civilian airports, vertiports, or in US airspace for commercial flight operations. For fixed-wing aircraft, AEDT calculates noise metrics using noise-power-distance (NPD) data provided by aircraft manufacturers. For a given flight path segment and receptor, these noise data are interpolated for engine power and distance to the receptor, and various adjustments are applied, to estimate the sound exposure at the receptor. For helicopters, AEDT uses noise-operating condition-distance curves, also provided by manufacturers, along with various adjustments, to estimate the

[1]stefan.j.letica@nasa.gov

[2]stephen.a.rizzi@nasa.gov

sound exposure at the receptor. These are similar to NPD curves, but the operating condition is specified directly via a procedural step [2]. This is because in contrast to fixed-wing mode, helicopter mode has no performance model and no correlating parameter (corrected net thrust) [1].

Prior work by the authors regarding AEDT has been performed in the context of assessing the use of AEDT as a software for modeling urban air mobility (UAM) vehicles and operations. The community noise impact of UAM vehicles could present an obstacle to the integration of these vehicles into society [3]. Much work has gone into developing tools to generate UAM source noise hemispheres and NPD data compatible with AEDT (see Ref. [4]). The means were developed to assess the noise exposure for point-to-point UAM operations for aircraft modeled as fixed-wing vehicles in AEDT [2, 5]. Subsequent work addressed modeling UAM vehicles as helicopter-type in AEDT and using those models for point-to-point operations, as well as mixtures of helicopter-type and fixed-wing-type operations [6]. These two approaches were shown to produce similar results in the flyover regime [2] but large differences were seen between AEDT fixed-wing and helicopter mode contours near takeoff and landing areas [6].

Noise contours around takeoff and landing areas are of elevated importance, as these are areas that will see high levels of activity and are where the greatest noise exposure occurs. Therefore, it is necessary to be able to estimate noise metrics in the vicinity of takeoff and landing areas with confidence. This paper explores and reports on the key differences between modeling vehicle operations in takeoff and landing areas using helicopter and fixed-wing modes in AEDT. Additionally, comparisons are made between AEDT contours and contours predicted by a NASA time-marching simulation tool.

2. METHODOLOGY

This section contains a brief description of the methods used to generate noise contours. Further details of the NASA source noise generation methodology and AEDT may be found in Refs. [4] and [2], respectively.

2.1. AEDT

AEDT is a Doc 9911-compliant [7] integrated noise modeling tool that is used to predict noise metrics and other environmental impacts associated with fixed-wing aircraft operations using noise-power-distance (NPD) data. AEDT also uses noise-operating condition-distance (also called NPD) data in helicopter mode. A key difference between fixed-wing and helicopter modes for this work is the number of unique operating conditions that can be specified for a particular operation.

The vehicle used in this work is the NASA RVLT reference quadrotor [8]. When modeling a UAM vehicle as a fixed-wing type, there are no performance data available to determine required engine power for interpolation of NPD data. Therefore, an approach was taken to use fixed-point flight profiles so that one can directly specify a full flight profile as a series of operational states. In helicopter mode, on the other hand, only a limited and specific series of operating conditions can be specified. In this work, modes L (level flyover), D (departure), and A (approach) are used, with substitutions following AEDT rules for all other operating conditions. For example, departure with horizontal acceleration, Mode E, is substituted with mode D. This severely limits the number of unique operational states that can be used when modeling an operation in helicopter mode.

Of particular importance to this work are the various adjustments to NPD data that AEDT makes to compute exposure-based metrics at ground receptors. These adjustments are given by Equation 1

for fixed-wing analyses, and Equation 2 for helicopter analyses [1].

$$E_{Seg,FW} = 10^{\frac{E_{NPD}+NF_{ADJ}+DUR_{ADJ}-LA_{ADJ}+TR_{ADJ}+DIR_{ADJ}}{10}} \quad (1)$$

$$E_{Seg,RW} = 10^{\frac{E_{NPD}+NF_{ADJ}+DUR_{ADJ}-LA_{ADJ}+MN_{ADJ}+LD_{ADJ}}{10}} \quad (2)$$

In Equations 1 and 2, E_{Seg} is the adjusted exposure-based metric calculated at the ground receptor, E_{NPD} is the interpolated NPD data based on the operating condition and distance to the receptor, NF_{ADJ} is the noise fraction adjustment, DUR_{ADJ} is the duration adjustment, LA_{ADJ} is the lateral attenuation adjustment, TR_{ADJ} and DIR_{ADJ} are the adjustments made for fixed-wing operations for thrust reverser deployment (approach) and takeoff roll noise directivity (departure), MN_{ADJ} is the advancing tip Mach number adjustment, and LD_{ADJ} is the helicopter lateral directivity adjustment, which interpolates NPD data for the receptor's relative elevation angle between the sidelines and centerline [1].

Of particular relevance to this work are the noise fraction adjustment, duration adjustment, and the lateral directivity adjustment. NPD data assume an infinitely long flight path segment; however, in practice, flight path segments are finite and AEDT computes each finite segment's contribution to the noise at a given receptor. The noise fraction adjustment computes this fraction of noise exposure from a finite path segment as a fourth-power 90° dipole model [9, 10]. Notably, the computation as performed in AEDT requires a reference speed to compute a scaled distance between the flight path segment and the observer. For fixed-wing vehicles, this is quite obvious, as all NPD data are provided with a reference speed of 160 knots. However, helicopter data are not typically provided at a reference speed of 160 knots.

The duration adjustment is an adjustment for exposure-based metrics that accounts for the speed difference between the NPD reference speed and the actual flight path segment speed, computed by a simple logarithmic ratio of the two speeds. Unlike the noise fraction adjustment, the reference speeds used are 160 knots for fixed-wing aircraft and the user-provided reference speed for the segment's given operational mode for helicopters [1].

The lateral directivity adjustment accounts for the directive sound radiation from helicopters based on sideline elevation angle between the receptor and the flight path. Helicopter NPD data for modes L, D, and A are provided at elevation angles of $\phi = 0$ and $\pm 45°$. The lateral directivity adjustment interpolates the data between these angles and uses the $\pm 45°$ data for angles greater than that [1]. The definition of ϕ is more clearly visualized in Figure 1.

The UAM vehicle is considered to be a propeller-driven aircraft when modeling it in AEDT as a fixed-wing type. This makes the lateral attenuation adjustment the same as that for helicopters and makes the thrust reverser adjustment equal to zero. Additionally, the advancing tip Mach number adjustment is not used in this work. Aside from the NPD data themselves, the remaining adjustments, i.e., noise fraction, duration, lateral directivity and (to a lesser extent) takeoff roll directivity, then contribute most to the differences between aircraft types and are a focus of the analyses that follow.

2.2. AMAT

The second-generation NASA Aircraft Noise Prediction Program (ANOPP2) [12] is a software framework for predicting aircraft noise and offers a number of tools and modules for doing so. One of these tools is the ANOPP2 Mission Analysis Tool (AMAT). AMAT is a time-marching simulation tool that uses ANOPP2 functional modules to simulate arbitrary flight paths using source noise hemispheres computed by the ANOPP2 Aeroacoustic Rotor Noise (AARON) tool. AMAT was used

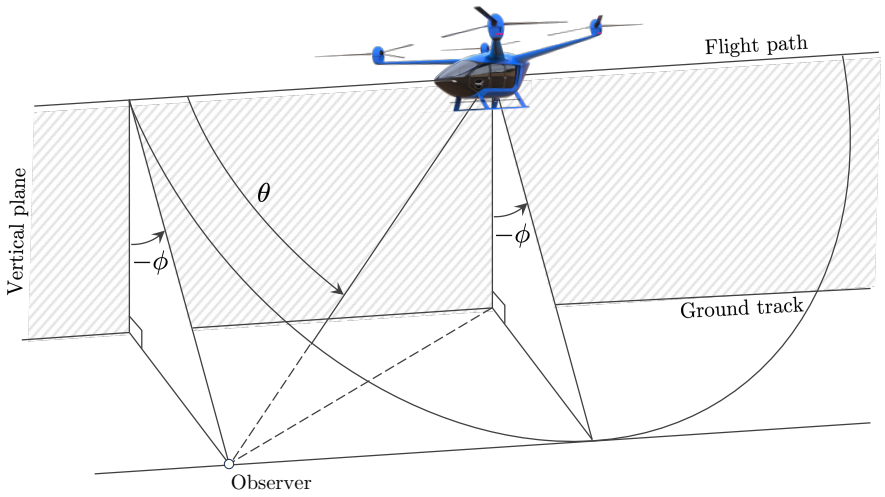

Figure 1: Definition of angles describing relative locations of flight path segment, vehicle, and receptors [11]. θ is referred to as 'polar angle', ϕ is referred to as 'sideline elevation angle'.

in Ref. [4] to compute NPD source noise data. In this work, the AMAT-simulated NPD data were used as AEDT inputs. The flights analyzed were also simulated directly using AMAT with the source noise data computed by AARON. In AMAT, the sound is propagated from the source to the observer using straight ray propagation and various noise metrics are produced for each ground observer.

2.3. Generation of NPD data

AMAT was used in Ref. [4] to generate NPD data for both fixed-wing and helicopter flight modes. The fixed-wing NPD data were computed using AARON source noise hemispheres flown straight and level at 160 knots, while the helicopter NPD data were computed using AARON source noise hemispheres flown directly at the specified operating condition (e.g., at 20 knots and 10° climb angle). Only modes A, D, and L (see above) were computed for the helicopter analyses, while all relevant operational states were used for the fixed-wing analyses. A more detailed discussion of why these data were chosen can be found in Refs. [2] and [4].

3. COMPARISONS BETWEEN AEDT FIXED-WING MODE AND HELICOPTER MODE

3.1. Baseline Comparison

To establish a starting point from which the analyses can be performed, with minimal AEDT adjustments, AEDT was run in both fixed-wing and helicopter modes for a simple overflight case. This run was performed with simulated NPD data for the NASA RVLT reference quadrotor (henceforth referred to as "quadrotor") at a speed of 90 knots, a climb angle of 0°, and an altitude of 1000 ft, over an extended west-to-east flight path. The flight is performed over flat sea-level terrain. The observers are a grid of AEDT receptors located at 4 feet above the ground. The bounds of the grid are ±1.5 miles, with a receptor spacing of 1/20 mi. The area examined was chosen to be much smaller in any dimension than the length of the total flight path to eliminate any end-of-segment

effects and ensure a steady operating condition for all receptors. The A-weighted sound exposure levels (SEL_A) of these runs are shown as contours in Figure 2.

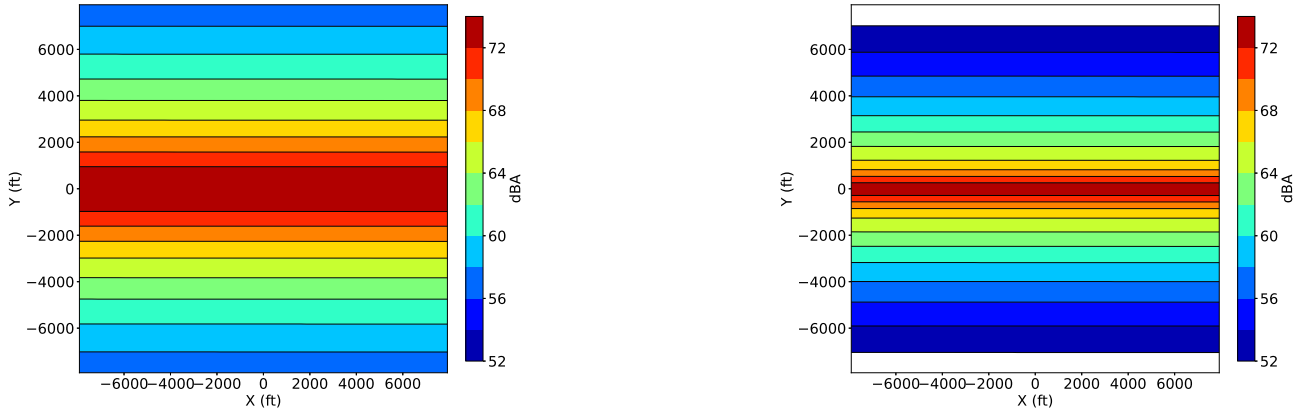

Figure 2: Baseline overflight noise exposure contours for fixed-wing mode (left) and helicopter mode (right), SEL_A.

Directly under the flight path (along $y = 0$), there is good agreement between the fixed-wing and helicopter mode contours; this shows that in areas where the lateral directivity adjustment is not applicable, the adjustments for duration and for noise fraction bring the separate helicopter and fixed-wing NPD data [4] together to provide a similar prediction for overflight. As can be clearly seen from Figure 2, however, the lateral directivity adjustment for helicopter analyses (Equation 2) creates large differences to the sides of the flight path.

The influence of the lateral directivity adjustment can be eliminated by setting the sideline NPD data for the helicopter analysis to be equal to the centerline NPD data (axisymmetric). The results of this analysis were then subtracted from the previous fixed-wing results. When this exercise was performed, it was found that the difference between the axisymmetric helicopter contours and the fixed-wing contours became negligible (not shown). This again indicates the ability of the duration and noise fraction adjustments to adequately adjust the separate helicopter and fixed-wing NPD data to provide a consistent prediction for both modes of analysis in overflight.

3.2. Approach Operation

To model an approach operation for the quadrotor, it was decided to use an existing helicopter approach profile within AEDT as the basis for the study. This profile was then modified such that only operational states for which NPD data exist for the quadrotor (see Ref. [4]) are used. This simplified approach also allows for a direct comparison between a fixed-wing and helicopter mode analysis of the same flight path, as conjugate NPD data for both fixed-wing and helicopter modes exist for all relevant operational states. To that end, the Bell 206 helicopter was chosen as a basis, which begins as a long segment of level flight, then a level deceleration, constant-velocity descent, and decelerating descent, before finally arriving with a brief segment of vertical descent. To more closely match the capabilities of the fixed-wing modeling scheme, the level deceleration, constant-velocity descent, and decelerating descent were modeled as a series of constant-operational state segments (no interpolation between states). The final segment of vertical descent from the Bell 206 was removed as it has negligible impact on the total noise exposure due to its short duration, and is not possible in

fixed-wing mode without introducing heavy distortion of contours [2]. Thus, the profile ends at an altitude of 15 ft. The approach profile is visualized in Figure 3.

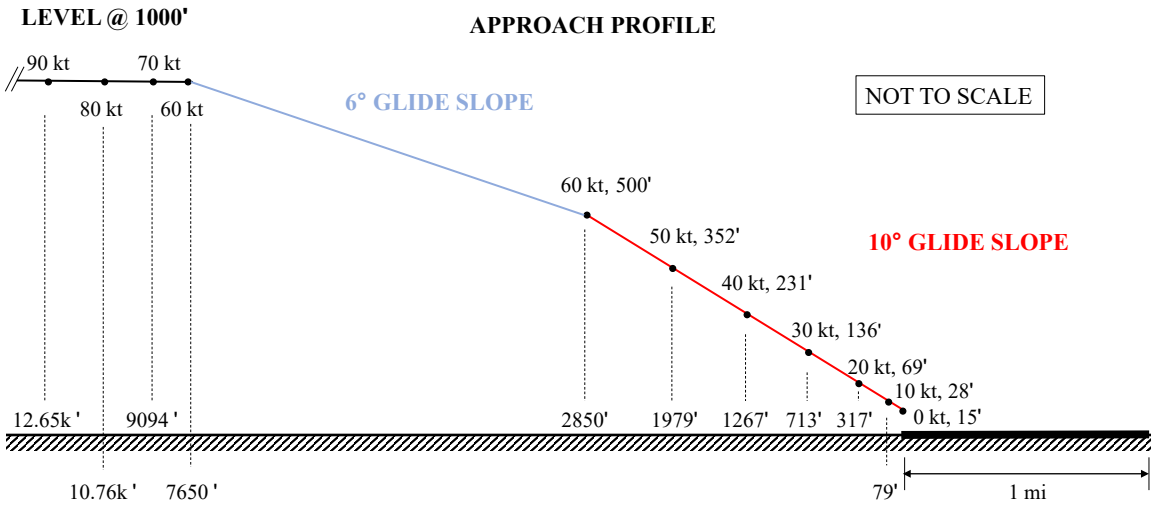

Figure 3: Profile for AEDT approach analyses. The heavy black horizontal line shows the extent of a one-mile runway with the landing point at the left (west) end. The center of this runway is located at $(x, y) = 0, 0$ ft, with positive x to the right (east).

The approach profile was run in AEDT in both helicopter and fixed-wing modes. In fixed-wing mode, all relevant operational states were used and guard points were included to ensure no interpolation occurred between operational states (see Ref. [2] for more details). In helicopter mode, operational modes L (90 kt, 0°) and A (20 kt, 10° descent) were used (see Ref. [4] for details on how these specific operational states were chosen). Figure 4 shows the contours of the approach analyses.

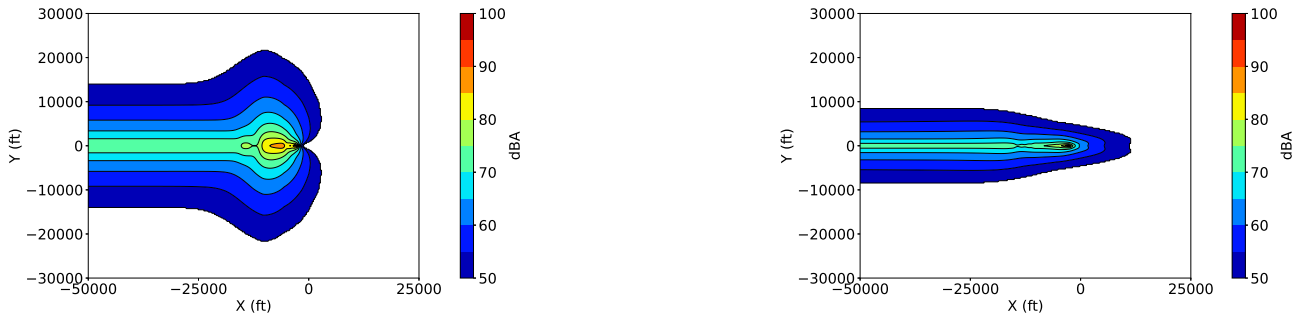

(a) Fixed-wing mode

(b) Helicopter mode

Figure 4: Baseline approach AEDT contours, SEL_A.

It is immediately obvious that there are large differences between the contours, especially around the landing site ($(x, y) = -2640, 0$ ft). To examine the sources of the differences, modifications were made to the two analyses to eliminate differences due to the source data. First, the fixed-wing analysis was run using only operational states present in the helicopter mode analysis; that is, all descent segments were replaced with the 20 knots, 10° descent NPD. Additionally, recall the previous section in which the helicopter NPD data were modified to be axisymmetric; the same technique was applied to the helicopter mode analysis here. In tandem, these two modified analyses should eliminate source

noise as the cause of the observed contour differences. Yet, as is clearly shown in Figure 5, there are still large differences in the shape of the contours. Both Figures 4a and 5a show a bulb-like shape, and both Figures 4b and 5b show an extended wedge-like shape.

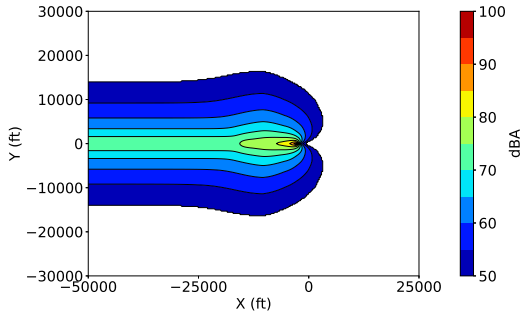

(a) Fixed-wing mode with two NPDs (helicopter-like)

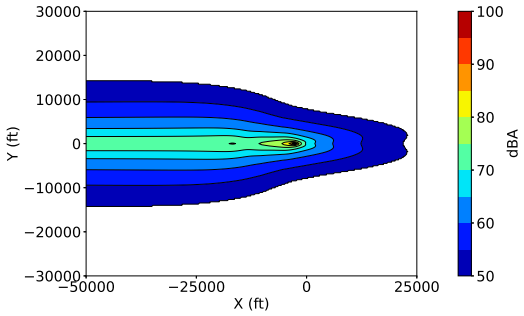

(b) Helicopter mode with axisymmetric NPD data (fixed-wing-like)

Figure 5: AEDT approach runs with modified source contours, SEL_A.

The differences between the two analyses are directly attributable to differences between the noise fraction calculation for helicopters and fixed-wing aircraft in the vicinity of an arrival airport. For fixed-wing vehicles, there is an additonal term added to the noise fraction calculation for receptors beyond the end of the last approach segment ($x > -2640$ ft) [1]. The results of plotting the adjustment associated with this additional term are shown in Figure 6. Note that the receptors in this grid are not in the same locations as those in the previous approach analyses. The figure indicates extra noise lobes to the northeast and southeast of the arrival point, which coincide with the lobes that make up the bulb-like shape shown in Figures 4a and 5a. It also explains why these lobes are not present in the helicopter analysis, resulting in the more wedge-like appearance.

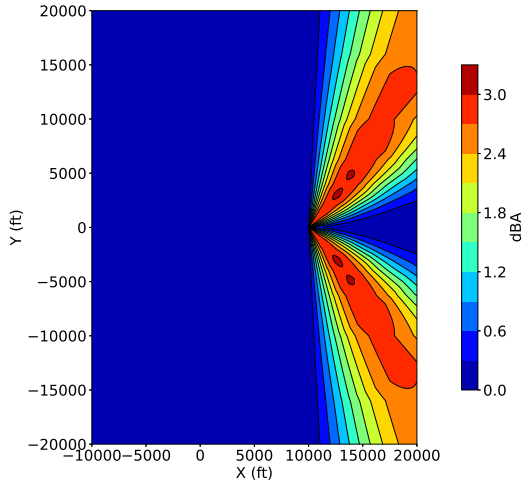

Figure 6: AEDT additional noise fraction adjustment for fixed-wing aircraft for points beyond the end of the approach flight path, dBA. In this figure, the end of the approach profile is at $x = 10560$ ft.

3.3. Departure Operation

Analyses analogous to those performed in Section 3.2 were performed for a nominal departure

operation. Again, the Bell 206 departure profile was used as a basis. As with the approach mode, the profile used for this analysis removed the vertical flight section, beginning the profile at an altitude of 15 ft. The helicopter analysis was also performed in the same manner as in Section 3.2, but instead of mode A (approach), mode D (departure) was used (20 knots, 10° ascent) [4]. The departure profile is visualized in Figure 7 and the results of these analyses are shown in Figure 8.

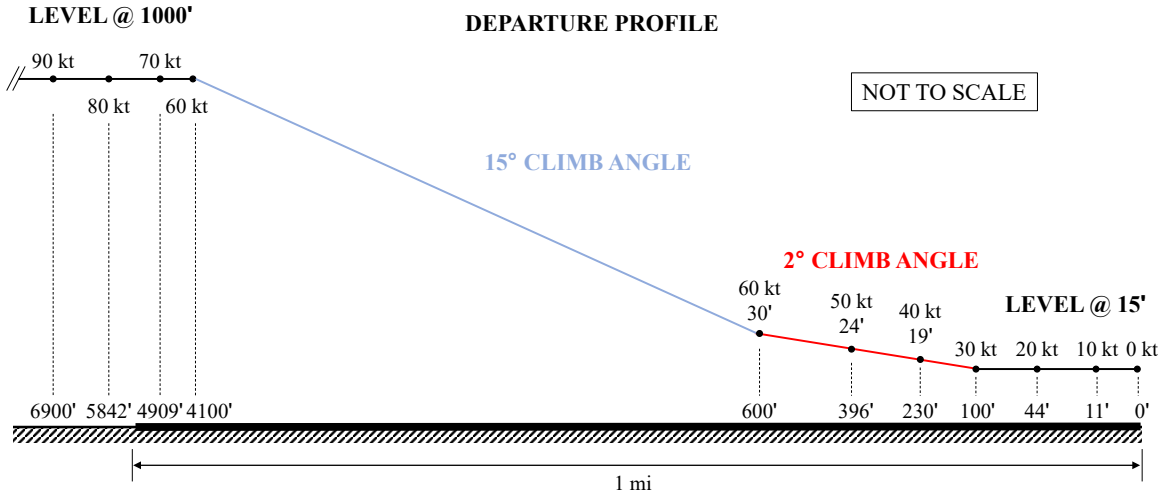

Figure 7: Profile for AEDT departure analyses. The heavy black horizontal line shows the extent of a one-mile runway with the departure point at the right (east) end. The center of this runway is located at $(x, y) = 0, 0$ ft, with positive x to the right.

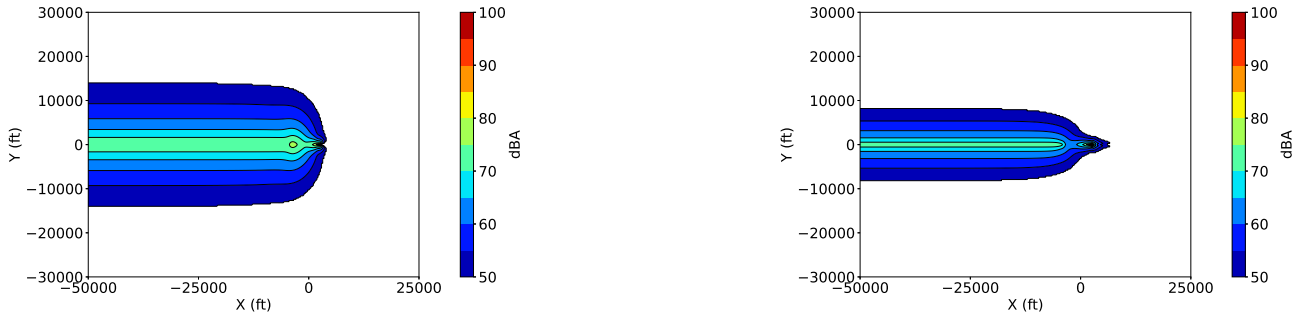

(a) Fixed-wing mode

(b) Helicopter mode

Figure 8: Baseline departure AEDT contours, SEL_A.

At first glance, it appears that there is better agreement between the helicopter and fixed-wing analyses for these nominal departure cases. However, there are still major differences in the overall width of the contours and the area in the vicinity of the departure point. To examine the source of these differences, the same modified analysis from Section 3.2 was repeated, using only 2 NPDs for the fixed-wing profile and using axisymmetric NPD data for the helicopter profile. The results of these analyses are shown in Figure 9.

There is better agreement between the modified approaches in Figure 9 than those in Figure 5. However, differences do still exist. These are attributable to both the noise fraction adjustment and the takeoff directivity adjustment (see Equation 1). Analogous to the approach case, there is an additional noise fraction adjustment for fixed-wing operations at receptors located behind the beginning of

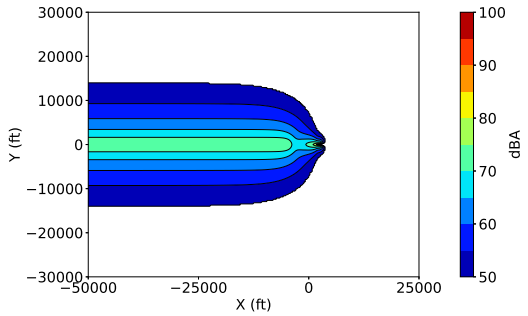

(a) Fixed-wing mode with two NPDs (helicopter-like)

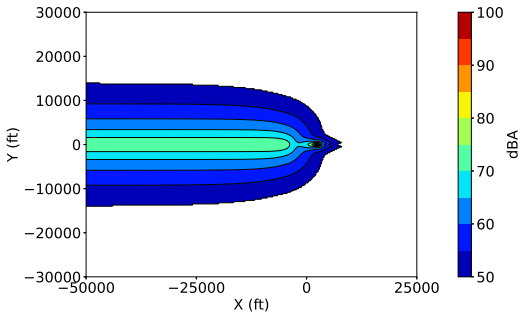

(b) Helicopter mode with axisymmetric NPD data (fixed-wing-like)

Figure 9: AEDT departure runs with modified source contours, SEL_A.

the first departure segment; when plotted, this adjustment looks similar to the beyond landing roll adjustment (Figure 6). Additionally, as this is a departure operation, the directivity adjustment DIR_{ADJ} is also applied to the fixed-wing contours shown in Figs. 8a and 9a. However, its full effect has not been thoroughly investigated. In any case, there are clear differences between helicopter and fixed-wing modeling in AEDT when it comes to the vicinity of takeoff and landing areas.

4. COMPARISONS BETWEEN AEDT AND AMAT

The previous analyses run in AEDT were also run using the NASA time-marching simulation tool AMAT. Care was taken to ensure that the AMAT analyses were run in as similar a manner as possible to the AEDT analyses to eliminate differences unrelated to the noise propagation methods and source noise; for exampe, for fixed-wing cases, AMAT was also run using 'guard points.' To that end, all vehicle operating states are exactly the same in the following AMAT runs as they are in the previously stated AEDT runs, unless otherwise specified. The authors do not maintain that the data predicted by AMAT are more 'truthful' than other predictions; rather, the AMAT data are used as a point of comparison to highlight how AEDT, an integrated noise model, compares to a time-marching simulation prediction method, especially in the regimes of approach and departure.

4.1. Overflight

First, a comparison of the two overflight runs from Section 3.1 was performed with an equivalent run performed in AMAT. This comparison is shown in Figure 10. It is clear from Figure 10 that directly under the flight path, the A-weighted SEL predicted by both helicopter and fixed-wing AEDT analyses compares favorably with that predicted by AMAT. In the region bounded by $\phi = \pm 45°$, i.e., $y = \pm 1000$ ft, the comparison between AEDT helicopter mode and AMAT is good because AEDT interpolates the helicopter NPD data over that range of angles. Outside of that region, the comparison is not as good. Because AEDT fixed-wing lacks the directivity adjustment, the results compare favorably only on the centerline.

4.2. Approach Comparison

Next, a comparison between the two AEDT approach runs and the equivalent profile run in AMAT was performed. This comparison is shown in Figure 11. For easier visualization, more detailed views

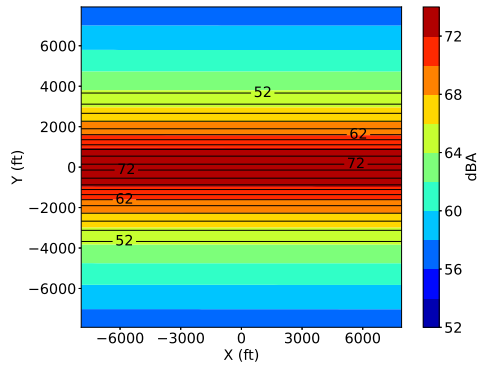

(a) Fixed-wing mode

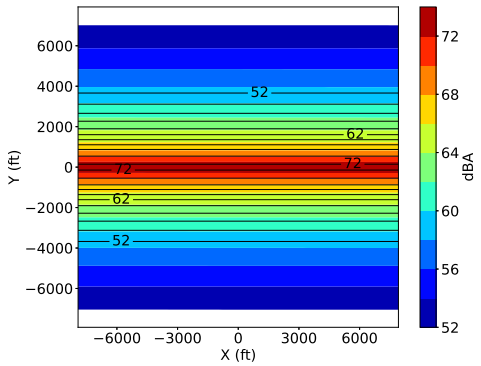

(b) Helicopter mode

Figure 10: Comparison of AEDT and AMAT overflight runs, SEL_A. Filled contours represent AEDT data and line contours represent AMAT data.

of the landing area are provided in Figures 11b and 11d.

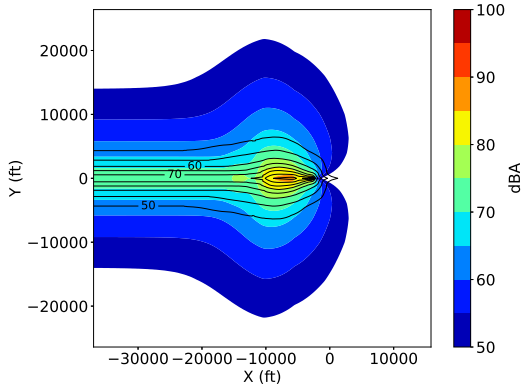

(a) Fixed-wing mode

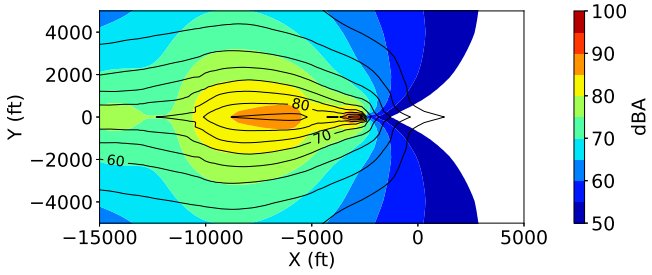

(b) Fixed-wing mode (zoomed)

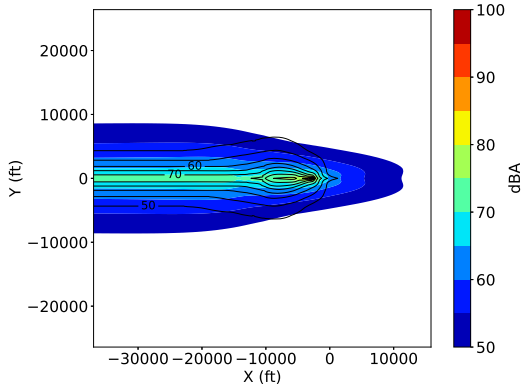

(c) Helicopter mode

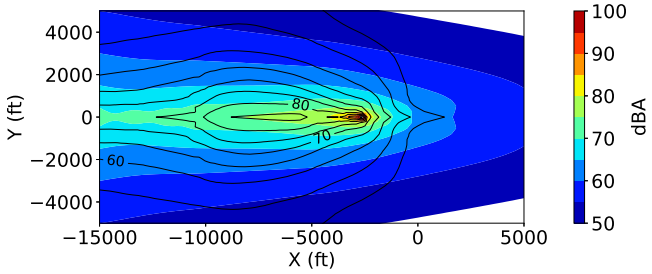

(d) Helicopter mode (zoomed)

Figure 11: Comparison of AEDT and AMAT approach runs, SEL_A. Filled contours represent AEDT data and line contours represent AMAT data.

In terms of overall contour width, the helicopter mode comparison to AMAT appears to be more favorable than the fixed-wing mode comparison, again attributable to the lateral directivity adjustment. However, as can be seen in the zoomed-in plots, there is a region of elevated SEL_A centered around

$x = -6500$ ft that is indicated by AMAT; the AEDT fixed-wing analysis captures this region, while the AEDT helicopter analysis does not. This is a consequence of using a single NPD for all descent segments of the flight profile in helicopter mode. Notably, this region is where the 6° glide slope region transitions into the 10° glide slope region in the approach profile (see Figure 3).

Generally, for regions above around 60 dBA, Figure 11 indicates that the fixed-wing analysis compares better to AMAT than the helicopter analysis. In addition, for receptors beyond the landing point, the AEDT helicopter analysis predicts much higher levels than indicated by AMAT and the AEDT fixed-wing analysis.

4.3. Departure Comparison

Finally, a comparison between the two AEDT departure runs and the equivalent profile run in AMAT was performed. This comparison is shown in Figure 12. For easier visualization, more detailed views of the landing area are provided in Figures 12b and 12d.

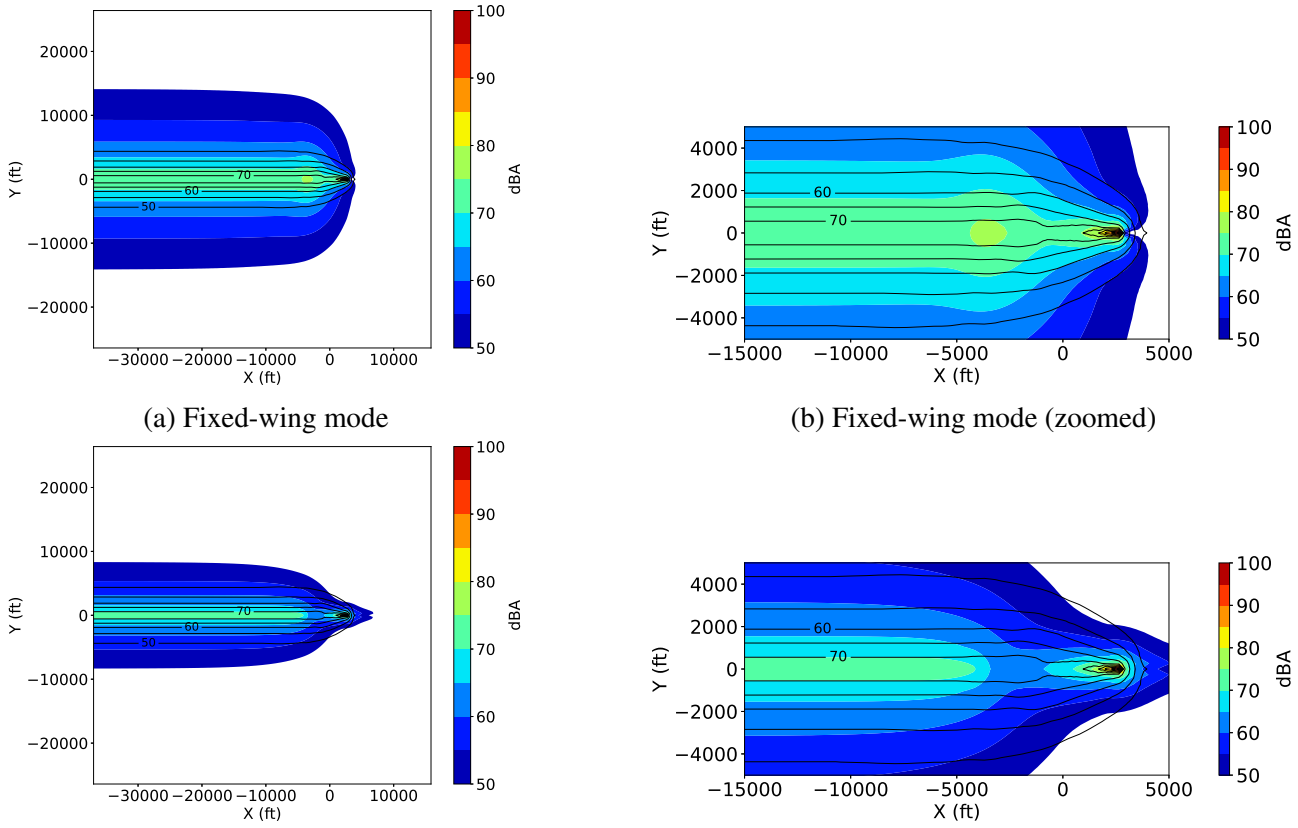

(a) Fixed-wing mode

(b) Fixed-wing mode (zoomed)

(c) Helicopter mode

(d) Helicopter mode (zoomed)

Figure 12: Comparison of AEDT and AMAT departure runs, SEL_A. Filled contours represent AEDT data and line contours represent AMAT data.

Again, the lateral directivity adjustment makes the comparison for points lateral to the flight path much more favorable for the helicopter analysis than for the fixed-wing analysis. As can be seen in the zoomed-in plots, however, there is a region of elevated SEL_A centered around $x = -4000$ ft that is indicated by AMAT; the fixed-wing analysis captures this region, while the helicopter mode analysis does not. Again, this is a consequence of using a single NPD for all ascent segments of the flight

profile in helicopter mode. This region is where the 15° ascent region transitions into the overflight region in the departure profile (see Figure 7).

Like the approach case, the comparison for regions above around 60 dBA is much better for the AEDT fixed-wing analysis. The favorable comparison for receptors east of the departure point for the fixed-wing analysis versus the helicopter analysis is also present. In aggregate, the comparisons between AEDT and AMAT are overall somewhat better for the departure cases than for the approach cases.

5. SUMMARY AND CONCLUSIONS

Comparisons were made between predicted A-weighted SEL data for AEDT analyses in fixed-wing mode, AEDT analyses in helicopter mode, and the NASA-developed time-marching simulation tool AMAT. It was found that both modes of AEDT analysis provided good comparisons to AMAT directly under the flight path in overflight mode, while astride the flight path, the lateral directivity adjustment applied in helicopter mode made comparisons for this mode more favorable than those for fixed-wing mode. The reasons for the differences between AEDT fixed-wing and helicopter mode analyses in the overflight regime are understood and documented and are primarily related to differences in the noise fraction calculation.

In the takeoff and landing regimes, it was found that the AEDT helicopter analysis did not adequately capture some features of the contours indicated by AMAT under the flight path, which the fixed-wing analysis did capture. This was because of the reduction of the number of unique operational states used in the helicopter analysis. In other areas around the takeoff and landing sites, especially to the sidelines, large differences were found between the two AEDT modes, neither of which were reflected in the simulation data.

The contribution of this work is to point out the sources of differences between different analysis methods in an effort to raise the awareness of practitioners. While there may be some obvious areas for improvements, the authors refrain from offering those here.

ACKNOWLEDGEMENTS

The authors would like to acknowledge Kevin P. Shepherd for his valuable contributions to their numerous internal discussions of AEDT and AMAT. This work is funded by the NASA Revolutionary Vertical Lift Technology (RVLT) project.

REFERENCES

[1] Aviation Environmental Design Tool (AEDT) Technical Manual, Version 3e. DOT-VNTSC-FAA-22-04, 2022.

[2] S. A. Rizzi and M. Rafaelof. Community noise assessment of urban air mobility vehicle operations using the FAA Aviation Environmental Design Tool. *INTER-NOISE and NOISE-CON Congress and Conference Proceedings*, 263:450–461, 8 2021.

[3] S. A. Rizzi et al. Urban air mobility noise: Current practice, gaps, and recommendations. Technical Memorandum TP-2020-5007433, NASA, 2020.

[4] S. A. Rizzi, S. J. Letica, D. D. Boyd, and L. V. Lopes. Prediction of noise-power-distance data for urban air mobility vehicles. *AIAA Journal of Aircraft*, 61:166–182, 1 2024.

[5] S. A. Rizzi and M. Rafaelof. Second generation UAM community noise assessment using the FAA Aviation Environmental Design Tool. *AIAA SCITECH 2022 Forum*. AIAA, 1 2022.

[6] S. A. Rizzi and M. Rafaelof. On the modeling of UAM aircraft community noise in AEDT helicopter mode. *AIAA AVIATION 2023 Forum*. AIAA, 6 2023.

[7] *Recommended Method for Computing Noise Contours Around Airports (Doc 9911)*. ICAO, 2nd edition, 2018.

[8] C. Silva, W. R. Johnson, E. Solis, M. D. Patterson, and K. R. Antcliff. VTOL urban air mobility concept vehicles for technology development. *2018 Aviation Technology, Integration, and Operations Conference*. AIAA, 2018.

[9] K. M. Eldred and R. L. Miller. Analysis of selected topics in the methodology of the Integrated Noise Model. Technical Report DOT-TSC-1782, US Department of Transportation, 1980.

[10] Doc 29 4th edition, Report on standard method of computing noise contours around civil airports volume 2: Technical guide. Technical report, ECAC, 2016.

[11] K. Pascioni, J. Page, and D. Boyle. UAM source noise hemisphere flight test measurement protocol. Technical Memorandum in review, NASA, 2024.

[12] L. V. Lopes and C. L. Burley. ANOPP2 User's Manual: Version 1.2. Technical Memorandum TM-2016-219342, NASA, 2016.